23rd ABCM International Congress of Mechanical Engineering
December 6-11, 2015, Rio de Janeiro, RJ, Brazil

INTEGRAL TRANSFORM SOLUTION FOR MAGNETOHYDRODYNAMIC FLOW WITH HEAT TRANSFER IN A PARALLEL-PLATE CHANNEL

Fabio de Andrade Pontes[1]
fabioapbelem@hotmail.com
Emanuel Negrão Macêdo[1]
enegrao@ufpa.br
Clauderino da Silva Batista[1]
clauderino@ufpa.br
João Alves de Lima[2]
jalima@cear.ufpb.br
João Nazareno Nonato Quaresma[1]
quaresma@ufpa.br
[1]Faculdade de Engenharia Química, Instituto de Tecnologia, Universidade Federal do Pará, PPGEQ/ITEC/UFPA, Campus Universitário do Guamá, 66075-110, Belém, PA, Brazil
[2]Departamento de Engenharia de Energias Renováveis, Centro de Energias Alternativas e Renováveis, Universidade Federal da Paraíba, DEER/CEAR/UFPB, Cidade Universitária, 58051-970, João Pessoa, PB, Brazil

Abstract. *The objective of present work is to apply the hybrid numerical/analytical approach known as GITT (Generalized Integral Transform Technique) by solving a magnetohydrodynamic flow of electrical conductor Newtonian fluids inside a parallel-plate channel subjected to a uniform and constant external magnetic field, wherein the mathematical formulation of the physical problem is given in terms of streamfunction obtained from the Navier-Stokes equations and the energy equation. The adopted assumptions are steady state, laminar and incompressible flow and constant physical properties. Convergence analyses are performed and presented in order to illustrate the consistency of the integral transformation technique. Results for the velocity and temperature fields are generated and compared with those in the literature as a function of the main governing parameters.*

Keywords: *Generalized Integral Transform Technique (GITT), Navier-Stokes equations, Magnetohydrodynamic (MHD), Heat transfer, Parallel-plates channel.*

1. INTRODUCTION

Magnetohydrodynamic (MHD) is the study of the interaction between electromagnetic and velocity fields of conductive fluids. Its mathematical modeling is characterized by the coupling between the fluid mechanics equations and the Maxwell's equations of electromagnetism. In the early twentieth century, it started studies on magnetohydrodynamics. From the 1960s until now, these studies have received considerable attention due mainly to energy and environmental issues. The fields of application in which the magnetohydrodynamic flow in channels with heat transfer are present include pumps and MHD generators, cooling systems of nuclear reactors and electrolytic reduction cells in aluminum plants (Shercliff, 1965; Davidson, 2001; Sutton and Sherman, 2006).

At the same time, there is a growing need for the development and application of mathematical methods that conserve a more analytical nature as much as possible in obtaining the solution of models in various science fields. Among the methodologies that satisfy this condition, at least partially, the so-called Generalized Integral Transform Technique (GITT), which is able to treat a large number of nonlinear problems, is an alternative tool for solving this class of problems. This technique is based on the use of orthogonal eigenfunction expansions to express the unknown dependent variables (Cotta, 1993; Cotta & Mikhailov, 1997; Cotta, 1998; Santos *et al*., 2001; Sphaier *et al.*, 2011).

The objective of this study is the application of this methodology in solving elliptical mathematical models in terms of streamfunction and temperature field simultaneously which governs such two-dimensional and incompressible flow with heat transfer in steady state of a Newtonian fluid. The mathematical model is obtained from the Navier-Stokes equations, the laws of electromagnetism and energy balance. The physical properties are constant and the flow is subjected to a transverse magnetic field, also constant.

2. ANALYSIS

2.1 Physical phenomenon

The problem addressed in this paper is defined by considering the magnetohydrodynamic flow with heat transfer in a channel formed by two parallel plates. It can be represented simply by a horizontal and semi-infinite rectangular duct. Within this channel flows an electric conductive fluid, subjected to a constant transverse magnetic field. Two of the four plates are isolated and the other two are electrodes, so that through them, an electric current can be imposed (pump), captured (generator), or they may be simply isolated (flowmeter). The plates, which are at different temperatures, transfers heat by convection to the fluid. Figure 1 shows the main characteristics of the flow and the geometry of the studied problem.

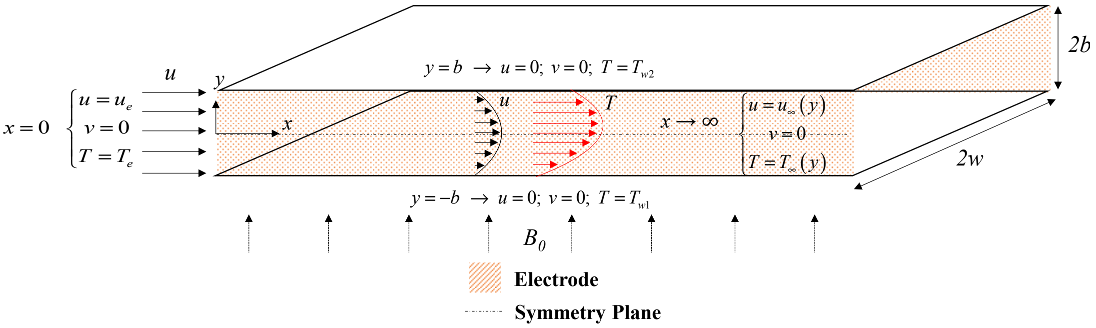

Figure 1. Geometric representation of the studied problem

From the simplifications adopted and given a formulation based on the Navier-Stokes equation, the governing equations of the flow with heat transfer problem in a parallel-plates channel with transverse magnetic field, in its dimensionless form, can be written as:

$$u\frac{\partial u}{\partial x}+v\frac{\partial u}{\partial y}=-\frac{\partial P}{\partial x}+\frac{4}{Re}\left(\frac{\partial^2 u}{\partial x^2}+\frac{\partial^2 u}{\partial y^2}\right)-\frac{4Ha^2}{Re}\left(E_0+u\right),\qquad 0<y<1,\ x>0 \tag{1}$$

$$u\frac{\partial v}{\partial x}+v\frac{\partial v}{\partial y}=-\frac{\partial P}{\partial y}+\frac{4}{Re}\left(\frac{\partial^2 v}{\partial x^2}+\frac{\partial^2 v}{\partial y^2}\right),\qquad 0<y<1,\ x>0 \tag{2}$$

$$u\frac{\partial T}{\partial x}+v\frac{\partial T}{\partial y}=\frac{4}{RePr}\left(\frac{\partial^2 T}{\partial x^2}+\frac{\partial^2 T}{\partial y^2}\right)+\frac{4Ec}{Re}\Phi+\frac{4EcHa^2}{Re}\left(E_0+u\right)^2,\qquad 0<y<1,\ x>0 \tag{3}$$

These equations are subjected to following boundary conditions:

$$x=0:\begin{cases}u=1\\ v=0\\ T=1\end{cases};\quad x\to\infty:\begin{cases}u=u_\infty(y)\\ v=0\\ T=T_\infty(y)\end{cases};\quad y=-1:\begin{cases}u=0\\ v=0\\ T=0\end{cases};\quad y=1:\begin{cases}u=0\\ v=0\\ T=T_{w21}\end{cases} \tag{4a-l}$$

In the above formulation, the following dimensionless groups were employed:

$$u=\frac{u^*}{U};\quad v=\frac{v^*}{U};\quad x=\frac{x^*}{b};\quad y=\frac{y^*}{b};\quad P=\frac{P^*}{\rho U^2};\quad \mathrm{Re}=\frac{4bU}{\nu};\quad Ha=B_0 b\left(\frac{\sigma}{\rho\nu}\right)^{1/2}$$
$$E_0=\frac{E_3^*}{UB_0};\quad T=\frac{T^*-T_{w1}}{T_e-T_{w1}};\quad T_{w21}=\frac{T_{w2}-T_{w1}}{T_e-T_{w1}};\quad \mathrm{Pr}=\frac{\nu}{\alpha}=\frac{\mu C_p}{k};\quad \mathrm{Ec}=\frac{U^2}{C_p\left(T_e-T_{w1}\right)} \tag{5a-l}$$

For the rectangular channel $D_h = 4b$. T_{w1} and T_{w2} are the bottom- and upper-plate temperatures. As both plates are at equal temperature, $T_{w1} = T_{w2}$ so $T_{w21} = 0$. E_3^* is the applied/extracted electric potential on the vertical walls (electrodes) while B_0^* is the applied constant vertical magnetic field. *Re*, *Pr*, *Ec* and *Ha* are the Reynolds, Prandtl, Eckert and Hartmann numbers, respectively.

2.2 Streamfunction-only formulation

In a previous research employing the GITT approach by Lima & Rêgo (2013), the use of streamfunction-only formulation showed more pronounced numerical convergence rates than those employing the primitive variable formulation. Thus, considering the streamfunction, $u=\partial\Psi/\partial y$ and $v=-\partial\Psi/\partial x$, Eqs. (1) to (3) subjected to boundary conditions (4a-l) are rewritten as:

$$\frac{\partial\Psi}{\partial y}\nabla^2\left(\frac{\partial\Psi}{\partial x}\right)-\frac{\partial\Psi}{\partial x}\nabla^2\left(\frac{\partial\Psi}{\partial y}\right)=\frac{4}{\mathrm{Re}}\nabla^4\Psi-\frac{4Ha^2}{\mathrm{Re}}\frac{\partial^2\Psi}{\partial y^2} \tag{6}$$

$$\frac{\partial\Psi}{\partial y}\frac{\partial T}{\partial x}-\frac{\partial\Psi}{\partial x}\frac{\partial T}{\partial y}=\frac{4}{RePr}\left(\frac{\partial^2 T}{\partial x^2}+\frac{\partial^2 T}{\partial y^2}\right)+\frac{4Ec}{\mathrm{Re}}\left[4\left(\frac{\partial^2\Psi}{\partial x\partial y}\right)^2+\left(\frac{\partial^2\Psi}{\partial y^2}-\frac{\partial^2\Psi}{\partial x^2}\right)^2\right]+\frac{4EcHa^2}{Re}\left(E_0+\frac{\partial\Psi}{\partial y}\right)^2 \quad (7)$$

These equations are subjected to the following inlet and boundary conditions:

$$x=0:\begin{cases}\Psi=1+y+C_1\\ \dfrac{\partial\Psi}{\partial x}=0\\ T=1\end{cases};\qquad x\to\infty:\begin{cases}\Psi=\Psi_\infty(y)\\ \dfrac{\partial\Psi}{\partial x}=0\\ T=T_\infty(y)\end{cases},\qquad y=-1:\begin{cases}\Psi=C_1\\ \dfrac{\partial\Psi}{\partial y}=0\\ T=0\end{cases},\qquad y=1:\begin{cases}\Psi=C_2\\ \dfrac{\partial\Psi}{\partial y}=0\\ T=T_{w21}\end{cases} \quad \text{(8a-l)}$$

2.3 Splitting of potentials

In order to improve the GITT performance and accelerate the convergence of the method, a splitting-up procedure is employed to remove non-homogeneous boundary conditions of the upper plate, where each original potential, $\Psi(x,y)$ and $T(x,y)$, is replaced by the filter functions as follows:

$$\Psi(x,y)=\Psi_\infty(y)+\Psi_F(x,y);\qquad T(x,y)=T_\infty(y)+T_F(x,y) \quad \text{(9a,b)}$$

By applying these definitions into Eqs. (6) and (7), subjected to the boundary conditions (8a-l), we get:

$$\frac{\partial\Psi_F}{\partial y}\nabla^2\left(\frac{\partial\Psi_F}{\partial x}\right)-\frac{\partial\Psi_F}{\partial x}\nabla^2\left(\frac{\partial\Psi_F}{\partial y}\right)+\frac{d\Psi_\infty}{dy}\nabla^2\left(\frac{\partial\Psi_F}{\partial x}\right)-\frac{\partial\Psi_F}{\partial x}\frac{d^3\Psi_\infty}{dy^3}=\frac{4}{Re}\nabla^4\Psi_F+\frac{4Ha^2}{Re}\frac{\partial^2\Psi_F}{\partial y^2} \quad (10)$$

$$\begin{aligned}&\frac{\partial\Psi_F}{\partial y}\frac{\partial T_F}{\partial x}-\frac{\partial\Psi_F}{\partial x}\frac{\partial T_F}{\partial y}+\frac{d\Psi_\infty}{dy}\frac{\partial T_F}{\partial x}-\frac{\partial\Psi_F}{\partial x}\frac{dT_\infty}{dy}=\frac{4}{RePr}\left(\frac{\partial^2 T_F}{\partial x^2}+\frac{\partial^2 T_F}{\partial y^2}\right)+\frac{4Ec}{Re}\left[4\left(\frac{\partial^2\Psi_F}{\partial x\partial y}\right)^2+\right.\\&\left.2\frac{d^2\Psi_\infty}{dy^2}\left(\frac{\partial^2\Psi_F}{\partial y^2}-\frac{\partial^2\Psi_F}{\partial x^2}\right)+\left(\frac{\partial^2\Psi_F}{\partial y^2}-\frac{\partial^2\Psi_F}{\partial x^2}\right)^2\right]+\frac{4EcHa^2}{Re}\left[\left(\frac{\partial\Psi_F}{\partial y}\right)^2+2\left(E_0+\frac{d\Psi_\infty}{dy}\right)\frac{\partial\Psi_F}{\partial y}\right]\end{aligned} \quad (11)$$

with the following boundary conditions:

$$x=0:\begin{cases}\Psi_F=1+y+C_1-\Psi_\infty(y)\\ \dfrac{\partial\Psi_F}{\partial x}=0\\ T_F=1-T_\infty(y)\end{cases};\qquad x\to\infty:\begin{cases}\Psi_F=0\\ \dfrac{\partial\Psi_F}{\partial x}=0\\ T_F=0\end{cases};\qquad y=-1:\begin{cases}\Psi_F=0\\ \dfrac{\partial\Psi_F}{\partial y}=0\\ T_F=0\end{cases};\qquad y=1:\begin{cases}\Psi_F=0\\ \dfrac{\partial\Psi_F}{\partial y}=0\\ T_F=0\end{cases} \quad \text{(12a-l)}$$

The exact fully developed velocity and temperature profiles were analytically obtained from one-dimensional problems, which bring the non-homogeneities in the boundary conditions, to yield:

$$\Psi_\infty(y)=\begin{cases}q+C_1+q\left(\dfrac{3y}{2}-\dfrac{y^3}{2}\right), & \textit{for Ha=0}\\[2ex] q+C_1+qK\left[y\cosh(Ha)-\dfrac{\sinh(Hay)}{Ha}\right], & \textit{for } Ha\neq 0\end{cases} \quad \text{(13a,b)}$$

$$T_\infty(y)=\begin{cases}\dfrac{T_{w21}}{2}(y+1)+\dfrac{3EcPrq^2}{4}\left(1-y^4\right), \quad \textit{for Ha=0}\\[2ex] \dfrac{T_{w21}}{2}(y+1)+EcHa^2Pr\left\{\dfrac{q^2K^2}{2Ha^2}\sinh^2(Ha)\left[1-\dfrac{\sinh^2(Hay)}{\sinh^2(Ha)}\right]\right.\\[2ex] \left.-\dfrac{2qK}{Ha^2}\cosh(Ha)\left[E_0+qK\cosh(Ha)\right]\left[1-\dfrac{\cosh(Hay)}{\cosh(Ha)}\right]+\dfrac{\left[E_0+qK\cosh\left(Ha\right)\right]^2}{2}\left(1-y^2\right)\right\}, \textit{for } Ha\neq 0\end{cases} \quad \text{(14a,b)}$$

where the constants C_1 and C_2 represent the values of the streamfunction at the duct walls, and q is a mass balance coefficient that warrants the global continuity, and it is related to C_1 and C_2 as follows below. Also, the constant K is defined as:

$$C_1 = C_2 + 2q\,; \qquad K = \frac{1}{\cosh(Ha) - \sinh(Ha)/Ha} \tag{15a,b}$$

2.4 Solution methodology: GITT approach

Since all boundary conditions are now homogeneous, the integral transformation of Eqs. (10) and (11) can be performed. The first step is to choose the eigenvalue problems. Such eigenvalue problems are obtained from homogeneous versions of the original problems, in the form:

2.4.1 For the streamfunction field

$$\frac{d^4\phi_i}{dy^4} = \mu_i^4 \phi_i\,, \qquad 0 < y < 1 \tag{16}$$

$$\phi_i(-1) = 0\,, \qquad \frac{d\phi_i(-1)}{dy} = 0\,, \qquad \phi_i(1) = 0\,, \qquad \frac{d\phi_i(1)}{dy} = 0 \tag{17a-d}$$

Therefore, the analytical solution for this eigenvalue problem is given by:

$$\phi_i(y) = \begin{cases} \dfrac{\cos(\mu_i y)}{\cos(\mu_i)} - \dfrac{\cosh(\mu_i y)}{\cosh(\mu_i)};\ i = 1,3,5,\ldots \\[2ex] \dfrac{\sin(\mu_i y)}{\sin(\mu_i)} - \dfrac{\sinh(\mu_i y)}{\sinh(\mu_i)};\ i = 2,4,6,\ldots \end{cases}, \qquad \tanh(\mu_i) = \begin{cases} -\tan(\mu_i);\ i = 1,3,5,\ldots \\ \tan(\mu_i);\ i = 2,4,6,\ldots \end{cases} \tag{18a-d}$$

$$\int_{-1}^{1} \phi_i(y)\phi_j(y)\,dy = \begin{cases} 0, & i \neq j \\ M_i, & i = j \end{cases}, \qquad M_i = \int_{-1}^{1} \phi_i^2(y)\,dy = 2\,, \qquad \tilde{\phi}_i(y) = \frac{\phi_i(y)}{\sqrt{M_i}} \tag{19a-d}$$

The eigenvalue above allows the definition of the following integral-transform pair:

$$\bar{\Psi}_i(x) = \int_{-1}^{1} \tilde{\phi}_i(y)\Psi_F(x,y)\,dy\,; \qquad \Psi_F(x,y) = \sum_{i=1}^{\infty} \tilde{\phi}_i(y)\bar{\Psi}_i(x) \tag{20a,b}$$

2.4.2 For the temperature field

$$\frac{d^2\Gamma_i}{dy^2} = -\alpha_i^2 \Gamma_i\,, \qquad 0 < y < 1 \tag{21}$$

$$\Gamma_i(-1) = 0, \qquad \Gamma_i(1) = 0 \tag{22a,b}$$

Similarly, the eigenfunctions, eigenvalues and the normalization integral are analytically obtained as:

$$\Gamma_i(y) = \sin[\alpha_i(y+1)]; \quad \alpha_i = \frac{i\pi}{2}, \quad i = 1,2,3,\ldots \tag{23a,b}$$

$$\int_{-1}^{1} \Gamma_i(y)\Gamma_j(y)\,dy = \begin{cases} 0, & i \neq j \\ N_i, & i = j \end{cases}, \qquad N_i = \int_{-1}^{1} \Gamma_i^2(y)\,dy = 1, \qquad \tilde{\Gamma}_i(y) = \frac{\Gamma_i(y)}{\sqrt{N_i}} \tag{24a-d}$$

Therefore, the integral-transform pair for the temperature field is then defined as:

$$\bar{T}_i(x) = \int_{-1}^{1} \tilde{\Gamma}_i(y) T_F(x,y)\,dy\,; \qquad T_F(x,y) = \sum_{i=1}^{\infty} \tilde{\Gamma}_i(y)\bar{T}_i(x) \tag{25a,b}$$

Finally, considering the eigenfunction orthogonality properties and boundary conditions, Eqs. (12), the integration of Eqs. (10) and (11), according to integral transform and inverse formulae, yields the following coupled system of ordinary differential equations in the x-direction:

$$\begin{aligned}\frac{d^4\bar{\Psi}_i(x)}{dx^4} &= -\mu_i^4\bar{\Psi}_i(x) - 2\sum_{j=1}^{\infty}A_{ij}\frac{d^2\bar{\Psi}_j(x)}{dx^2} + \frac{Re}{2}\left\{\sum_{j=1}^{\infty}\sum_{k=1}^{\infty}\left[B_{ijk}\frac{d^3\bar{\Psi}_j(x)}{dx^3}\bar{\Psi}_k(x) + \right.\right.\\ &\left. + C_{ijk}\bar{\Psi}_j(x)\frac{d\bar{\Psi}_k(x)}{dx} - D_{ijk}\frac{d\bar{\Psi}_j(x)}{dx}\bar{\Psi}_k(x) - B_{ijk}\frac{d\bar{\Psi}_j(x)}{dx}\frac{d^2\bar{\Psi}_k(x)}{dx^2}\right] + \\ &\left. + \sum_{j=1}^{\infty}\left[E_{ij}\frac{d^3\bar{\Psi}_j(x)}{dx^3} + F_{ij}\frac{d\bar{\Psi}_j(x)}{dx} - G_{ij}\frac{d\bar{\Psi}_j(x)}{dx}\right]\right\}\end{aligned} \qquad i = 1,2,3,\ldots,\infty \quad (26)$$

$$\begin{aligned}\frac{d^2\bar{T}_i(x)}{dx^2} &= -\alpha_i^2\bar{T}_i(x) + \frac{RePr}{4}\sum_{j=1}^{\infty}\sum_{k=1}^{\infty}H_{ijk}\frac{d\bar{T}_j(x)}{dx}\bar{\Psi}_k(x) - \sum_{j=1}^{\infty}\sum_{k=1}^{\infty}I_{ijk}\bar{T}_j(x)\frac{d\bar{\Psi}_k(x)}{dx}\\ &+ \sum_{j=1}^{\infty}J_{ij}\frac{d\bar{T}_j(x)}{dx} - \sum_{j=1}^{\infty}K_{ij}\frac{d\bar{\Psi}_j(x)}{dx} - EcPrL_i(x)\end{aligned} \qquad i = 1,2,3,\ldots,\infty \quad (27)$$

The boundary conditions in the x-direction are similarly integral-transformed, to yield:

$$\bar{\Psi}_i(0) = \int_{-1}^{1}\tilde{\phi}_i(y)\left[1 + y + C_1 - \Psi_\infty(y)\right]dy\,; \quad \frac{d\bar{\Psi}_i(0)}{dx} = 0\,; \quad \bar{T}_i(0) = \int_{-1}^{1}\tilde{\Gamma}_i(y)\left[1 - T_\infty(y)\right]dy \qquad (28a\text{-}c)$$

$$\bar{\Psi}_i(\infty) = 0\,; \quad \frac{d\bar{\Psi}_i(\infty)}{dx} = 0\,; \quad \bar{T}_i(\infty) = 0 \qquad (28d\text{-}f)$$

The above coefficients, resulting from the integral transformation process, are defined as:

$$A_{ij} = \int_{-1}^{1}\tilde{\phi}_i(y)\tilde{\phi}_j''(y)dy\,; \quad B_{ijk} = \int_{-1}^{1}\tilde{\phi}_i(y)\tilde{\phi}_j(y)\tilde{\phi}_k'(y)dy\,; \quad C_{ijk} = \int_{-1}^{1}\tilde{\phi}_i(y)\tilde{\phi}_j'(y)\tilde{\phi}_k''(y)dy \qquad (29a\text{-}c)$$

$$D_{ijk} = \int_{-1}^{1}\tilde{\phi}_i(y)\tilde{\phi}_j(y)\tilde{\phi}_k'''(y)dy\,; \quad E_{ij} = \int_{-1}^{1}\tilde{\phi}_i(y)\tilde{\phi}_j(y)\frac{d\Psi_\infty(y)}{dy}dy\,; \quad F_{ij} = \int_{-1}^{1}\tilde{\phi}_i(y)\tilde{\phi}_j''(y)\frac{d\Psi_\infty(y)}{dy}dy \qquad (29d\text{-}f)$$

$$G_{ij} = \int_{-1}^{1}\tilde{\phi}_i(y)\tilde{\phi}_j(y)\frac{d^3\Psi_\infty(y)}{dy^3}dy\,; \quad H_{ijk} = \int_{-1}^{1}\tilde{\Gamma}_i(y)\tilde{\Gamma}_j(y)\tilde{\phi}_k'(y)dy\,; \quad I_{ijk} = \int_{-1}^{1}\tilde{\Gamma}_i(y)\tilde{\Gamma}_j'(y)\tilde{\phi}_k(y)dy \qquad (29g\text{-}i)$$

$$J_{ij} = \int_{-1}^{1}\tilde{\Gamma}_i(y)\tilde{\Gamma}_j(y)\frac{d\Psi_\infty(y)}{dy}dy\,; \quad K_{ij} = \int_{-1}^{1}\tilde{\Gamma}_i(y)\tilde{\phi}_j(y)\frac{dT_\infty(y)}{dy}dy \qquad (29j,k)$$

$$L_i = \int_{-1}^{1}\tilde{\Gamma}_i(y)\left\{4\left(\frac{\partial^2\Psi_F}{\partial x\partial y}\right)^2 + 2\frac{d^2\Psi_\infty}{dy^2}\left(\frac{\partial^2\Psi_F}{\partial y^2} - \frac{\partial^2\Psi_F}{\partial x^2}\right) + \left(\frac{\partial^2\Psi_F}{\partial y^2} - \frac{\partial^2\Psi_F}{\partial x^2}\right)^2 + Ha^2\left[\left(\frac{\partial\Psi_F}{\partial y}\right)^2 + 2\left(E_0 + \frac{d\Psi_\infty}{dy}\right)\frac{\partial\Psi_F}{\partial y}\right]\right\}dy \qquad (29l)$$

3. RESULTS AND DISCUSSION

To obtain the numerical results a computer code was developed in FORTRAN 90 language. The DBVPFD subroutine, from the scientific library IMSL (2010), was used, which is especially suitable for solving systems of ordinary differential equations with stiff characteristics, such as the system found in the present study.

The convergence analyses of the integral transform technique was performed in order to evaluate the influence of the gradual increase process in truncation order of the series (expansions), until a certain criterion of numerical error in the numerical results (velocity and temperature fields, velocity and temperature gradients, the product of the friction factor by the Reynolds number (*fRe*) and local Nusselt number) has been reached. The convergence of the velocity and temperature fields was analyzed at the central plane of the channel (y=0), whereas for the product *fRe* (which is a function of the velocity gradient) and the local Nusselt number (which is a function of the temperature gradient) was performed at the upper plate (y = 1), both in specific values of the longitudinal coordinates.

Table 1 illustrates the convergence behavior by considering Re = 300; Ha = 10; Pr = 0.75; E_0 = -0.5; Ec = 0.1 (with viscous dissipation and Joule heating) and T_{w21} = 0.0. From this table, it is noted that the convergence rates for velocity and temperature fields were considered very good, since, with few terms in the series, they are already substantially converged within four significant digits, even to flow regions very close to the channel entry. In contrast, convergence rates were not so good for the gradients, particularly the velocity gradient and as a consequence for the product *fRe*, so that for these fields more than 71 terms are needed for the convergence of three significant digits, especially at the channel entry ($x = 0.2$ and $x = 0.4$), although the temperature gradient and the local Nusselt number present convergence with fewer terms in the series.

Table 2 illustrates the convergence behavior by considering $Re = 100$; $Ha = 4$; $Pr = 1.0$; $Ec = 0.0$ (without viscous dissipation and without Joule heating); $E_0 = 0.0$ and $T_{w21} = 0.0$. The convergence for the velocity and temperature fields presented in Tab. 2 occurs at an accelerated rate.

Table 1. Convergence behavior of the results in different axial positions, for $Re = 300$; $Ha = 10$; $Pr = 0.75$; $Ec = 0.1$; $E_0 = -0.5$ and $T_{w21} = 0.0$.

N \ x	$u_c(x)$				$T_c(x)$				$\partial u/\partial y\|_{y=1}$			
	0.2	0.4	0.6	0.8	0.2	0.4	0.6	0.8	0.2	0.4	0.6	0.8
11	0.9794	1.0142	1.037	1.056	0.9936	1.013	1.023	1.031	19.97	15.47	13.03	11.89
23	1.006	**1.019**	**1.038**	1.056	**1.007**	**1.014**	**1.021**	**1.029**	21.35	13.88	12.15	11.52
35	1.006	**1.019**	**1.038**	**1.057**	**1.007**	**1.014**	**1.021**	**1.029**	19.58	13.66	12.12	**11.51**
47	**1.005**	**1.019**	**1.038**	**1.057**	**1.007**	**1.014**	**1.021**	**1.029**	19.05	13.63	**12.11**	**11.51**
59	**1.005**	**1.019**	**1.038**	**1.057**	**1.007**	**1.014**	**1.021**	**1.029**	18.92	**13.62**	**12.11**	**11.51**
71	**1.005**	**1.019**	**1.038**	**1.057**	**1.007**	**1.014**	**1.021**	**1.029**	18.86	**13.62**	**12.12**	**11.51**
N \ x	$\partial T/\partial y\|_{y=1}$				*fRe*				Nu_1			
	0.2	0.4	0.6	0.8	0.2	0.4	0.6	0.8	0.2	0.4	0.6	0.8
11	9.183	7.23	6.012	5.242	159.8	123.7	104.25	95.09	37.73	29.98	25.11	22.03
23	10.38	7.161	5.86	5.121	170.8	111.1	97.20	92.15	42.72	29.74	24.52	21.58
35	10.19	7.094	5.819	5.094	156.7	109.3	96.93	92.08	42.00	29.48	24.37	21.48
47	10.14	7.074	5.807	5.085	152.4	**109.0**	96.91	92.09	41.8	29.41	24.33	21.45
59	**10.13**	**7.068**	5.804	5.082	151.3	**109.0**	96.92	92.1	**41.76**	**29.40**	**24.32**	**21.44**
71	**10.13**	**7.068**	5.803	5.081	150.9	**109.0**	96.93	92.11	**41.76**	**29.40**	**24.32**	**21.44**

Table 2. Convergence behavior of the results in different axial positions for $Re = 100$; $Ha = 4$; $Pr = 1.0$; $Ec = 0.0$; $E_0 = 0.0$ and $T_{w21} = 0.0$.

N \ x	$u_c(x)$				$T_c(x)$				$\partial u/\partial y\|_{y=1}$			
	0.1	1.0	2.0	5.0	0.1	1.0	2.0	5.0	0.1	1.0	2.0	5.0
11	0.9580	1.159	**1.260**	**1.284**	0.9845	0.9989	0.9705	0.7943	19.84	5.809	**5.366**	**5.329**
23	0.9979	**1.161**	**1.260**	**1.284**	0.9992	0.9972	0.9678	0.7912	26.56	5.778	**5.366**	**5.329**
35	**1.003**	**1.161**	**1.260**	**1.284**	**1.000**	0.9970	0.9674	0.7908	26.62	**5.777**	**5.366**	**5.329**
47	**1.003**	**1.161**	**1.260**	**1.284**	**1.000**	**0.9969**	0.9673	0.7907	25.72	**5.777**	**5.366**	**5.329**
59	**1.003**	**1.161**	**1.260**	**1.284**	**1.000**	**0.9969**	**0.9672**	**0.7906**	25.08	**5.777**	**5.366**	**5.329**
71	**1.003**	**1.161**	**1.260**	**1.284**	**1.000**	**0.9969**	**0.9672**	**0.7906**	24.72	**5.777**	**5.366**	**5.329**
N \ x	$\partial T/\partial y\|_{y=1}$				*fRe*				Nu_1			
	0.1	1.0	2.0	5.0	0.1	1.0	2.0	5.0	0.1	1.0	2.0	5.0
11	8.486	2.341	1.746	1.205	158.7	46.47	**42.93**	**42.63**	35.58	11.31	9.300	8.292
23	9.788	2.308	1.732	1.199	212.5	**46.22**	**42.93**	**42.63**	41.44	11.20	9.264	8.284
35	9.658	2.303	1.730	**1.198**	213.0	**46.22**	**42.93**	**42.63**	40.95	**11.18**	9.258	**8.283**
47	9.541	2.302	**1.729**	**1.198**	205.8	**46.22**	**42.93**	**42.63**	40.47	**11.18**	**9.257**	**8.283**
59	9.492	**2.301**	**1.729**	**1.198**	200.6	**46.22**	**42.93**	**42.63**	40.26	**11.18**	**9.256**	**8.283**
71	9.472	**2.301**	**1.729**	**1.198**	197.8	**46.22**	**42.93**	**42.63**	40.18	**11.18**	**9.256**	**8.283**

Here, it is also highlighted that four parameters related to the original fields show a convergence only at the third significant digit, so that, as in the previous case, a more accurate convergence to a higher number of terms ($N > 71$) must be used. It is noteworthy that in this case we used the point $x = 5$, where most of the parameters analyzed have accelerated convergence to the required significant digits.

Figures 2 and 3 have the purpose to verify the results of the present methodology for the axial component along the channel at different transverse positions (y) against those results of Manohar (1966) and Lima & Rêgo (2013) ($Re = 100$ and $Ha = 4$) and Manohar (1966) ($Re = 300$ and $Ha = 10$), and for the development of the velocity profile in some longitudinal positions (x) with the data of Lima & Rêgo (2013) ($Re = 100$ and $Ha = 4$ and $Re = 300$ and $Ha = 10$). Note that Manohar (1966) applied finite differences method with a boundary layer formulation in their studies (referenced in the figures by BL/FDM), while Lima & Rêgo (2013) applied Generalized Integral Transform Technique with a boundary layer formulation in their work (referenced in the figures by BL/GITT).

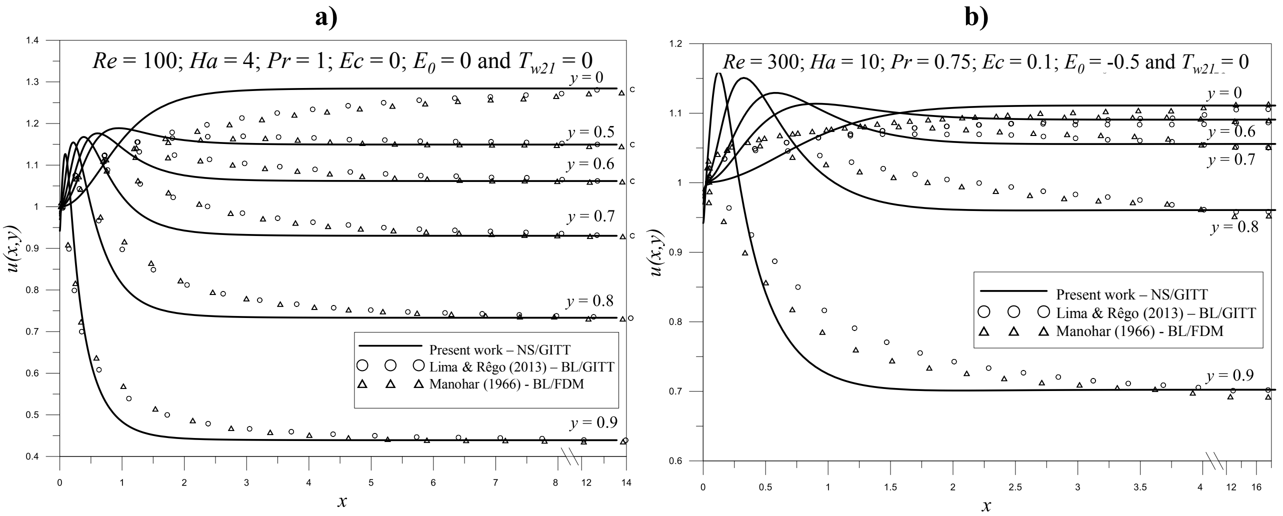

Figure 2. Comparison of the present results for the axial velocity component along the channel at different transverse positions with those of: a) Manohar (1966) and Lima & Rêgo (2013) for $Re = 100$ and $Ha = 4$; b) Manohar (1966) and Lima & Rêgo (2013) for $Re = 300$ and $Ha = 10$.

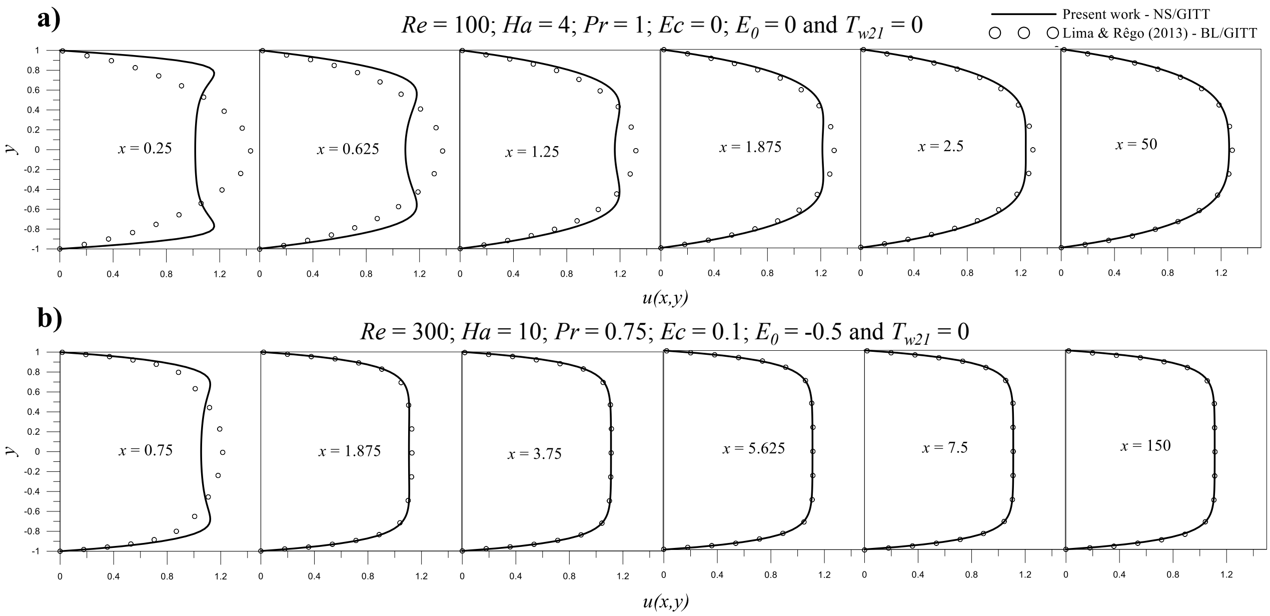

Figure 3. Comparison of the present results with those of Lima & Rêgo (2013) for the development of the velocity profile (axial component) along the channel for: a) $Re = 100$ and $Ha = 4$; b) $Re = 300$ and $Ha = 10$.

From Figs. 2 and 3, it can be said that the present results for the axial velocity field along the channel were satisfactorily checked with those of Manohar (1966) and Lima & Rêgo (2013) since these profiles have an excellent overall agreement in the regions away from the entrance, although velocity profiles exhibit the “overshooting” phenomenon near the walls at the channel entrance. The velocity overshootings arise on account of a negative pressure gradient established near the wall in a very short distance region from the channel inlet (x = 0), while a positive pressure gradient exists in the region near the centerline (y = 0). Therefore, flow near this position is not immediately accelerated and the velocity overshootings are formed (Sparrow, 1964). This overshooting behavior is not captured by mathematical models that use Boundary Layer Formulation (BLF), as those studies by Manohar (1966) and Lima & Rêgo (2013). On the contrary, this effect is only incorporated when all viscous force terms are maintained in the Navier-Stokes equations (NS) in their most complete form as employed in the present work.

In Fig. 4, it can be observed an excellent agreement between the results for the development of the velocity profile (axial component) of present work with the results of Lima & Rêgo (2013) for the case of Re = 40 and Ha = 50. It is noteworthy that for high values of Hartmann number (Ha = 50), as in this case, the development of the velocity field shows a planned profile. It is again observed the same behavior profile at the channel entrance (overshooting), and it can be said that this is closer to the actual behavior of the flow, due to the more complete formulation used in this study.

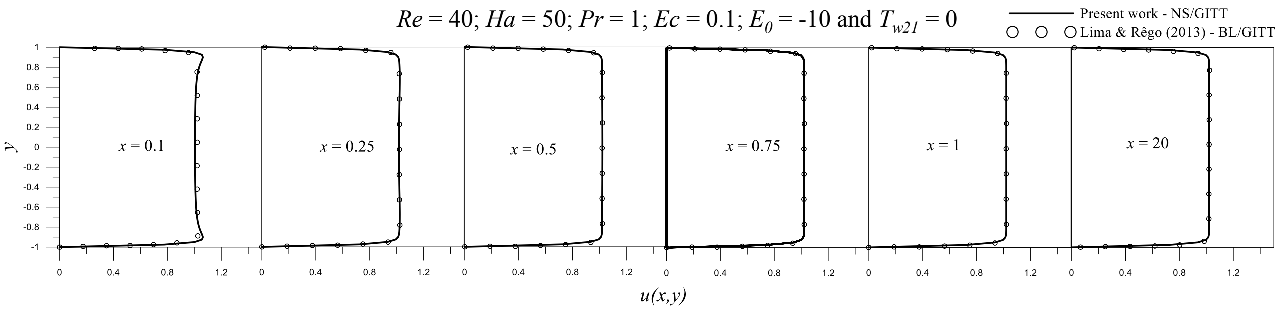

Figure 4. Comparison of the present results with those of Lima & Rêgo (2013) for the velocity profile development (axial component) along the channel for Re = 40 and Ha = 50.

4. CONCUSIONS

The verification of results performed in comparison with those of other authors (obtained from numerical or hybrid methods) were considered satisfactory, so that the computer code developed can be employed for depth investigation of the cases evaluated here and further on the effects and conditions over the flow and heat transfer in the channel.

The GITT proved to be a robust and versatile technical solution for the nonlinear problem here stated, therefore enabling the extent of the same solution of this class of problems which involve electromagnetic phenomena.

It is remarkable that the applied technique (GITT) along with the type of full MHD formulation (Navier-Stokes equations), had not yet been the subject of previous work, representing an expansion of the application of the methodology and results, considered more generic because they take into account the input effects disregarded in prior works.

5. REFERENCES

COTTA, R.M. Integral Transform in Computational Heat and Fluid. CRC Press, Boca Rator, FL, 1993.

COTTA, R.M.; MIKHAILOV, M.D. Heat Conduction: Lumped Analysis, Integral transforms, Symbolic Computation, John Wiley & Sons, 1997.

COTTA, R.M. The Integral Transform Method in Thermal and Fluids Sciences and Engineering, Beggel House, NY, USA, 1998.

DAVIDSON, P.A. An Introduction to Magnetohydrodynamics. Cambridge University Press, Cambridge, UK, 2001.

IMSL LIBRARY, Rogue Wave Software, Visual Numerics. Boulder, Colorado, 2010.

LIMA, J.A.; QUARESMA, J.N.N. & NEGRÃO, E.N. Integral transform analysis of MHD flow and heat transfer in parallel-plates channels. International Communications in Heat and Mass Transfer 34. 420–431, 2007.

LIMA, J.A. & RÊGO, M.G.O. On the integral transform solution of low-magnetic MHD flow and heat transfer in the entrance region of a channel. International Journal of Non-Linear Mechanics, 50, 25–39, 2013.

MANOHAR, R. An Exact Analysis of Laminar Magnetohydrodynamic Flow in the Entrance Region of a Flat Duct. Journal of Applied Mathematics and Mechanics / Zeitschrift für Angewandte Mathematik und Mechanik - ZAMM, vol. 46, no 2, pp. 111-117, 1966.

SHERCLIFF, J.A. A Textbook of Magnetohydrodynamics, Pergamon Press, London, UK, 1965.

SANTOS, C.A.C.; QUARESMA, J.N.N. & LIMA, J.A. Convective Heat Transfer in Ducts: the Integral Transform Approach, 348p., E-Papers, ABCM Mechanical Sciences Series, Rio de Janeiro, Brazil, 2001.

SPARROW, E.M.; LIN, S.H. & LUNDGREN, T.S. Flow Development in the Hydrodynamic Entrance Region of Tubes and Ducts, The Physics of Fluids, vol. 7, no 3, pp. 338-347, 1964.

SPHAIER, L. A.; COTTA, R. M.; NAVEIRA-COTTA, C. P.; QUARESMA, J. N. N. The UNIT algorithm for solving one-dimensional convection-diffusion problems via integral transforms. I. C. Heat and Mass Transfer. v. 38, p. 565-571, 2011.

SUTTON, G.W. & SHERMAN, A. Engineering Magnetohydrodynamics, Dover Publications, Inc, Mineola, New York, USA, 2006.

6. RESPONSIBILITY NOTICE

The authors are the only responsible for the printed material included in this paper.